Research Article | Vol. 27, No. 15 | 22 Jul 2019 | OPTICS EXPRESS 20848
Optics EXPRESS

Two-dimensional vector accelerometer based on Bragg gratings inscribed in a multi-core fiber

JINGXIAN CUI,[1] ZHENGYONG LIU,[1,*] DINUSHA SERANDI GUNAWARDENA,[1] ZHIYONG ZHAO,[2] AND HWA-YAW TAM[1]

[1]*Photonics Research Centre, Department of Electrical Engineering, The Hong Kong Polytechnic University, Hung Hom, Kowloon, Hong Kong, China*
[2]*Photonics Research Centre, Department of Electronic and Information Engineering, The Hong Kong Polytechnic University, Hung Hom, Kowloon, Hong Kong, China*
**zhengyong.liu@connect.polyu.hk*

Abstract: We propose and demonstrate a novel orientation-sensitive two-dimensional accelerometer based on fiber Bragg gratings inscribed in a multi-core fiber. Through monitoring of the wavelength shifts of three of the seven cores, including the central core and two outer cores which are not aligned in a straight line, information on vibration orientation as well as acceleration can be obtained simultaneously. Performance of the proposed accelerometer in terms of frequency, acceleration and vibration orientation are experimentally investigated. The designed two-dimensional accelerometer is capable of obtaining all these three parameters simultaneously. A sensitivity which is strongly dependent on the orientation is achieved, with a best orientation accuracy of 0.127° over a range of 0-180°. Moreover, the resonance frequency and the sensitivity can be optimized through adjusting the length and weight of the free-fiber. The ease of fabrication as well as the versatility of the proposed sensor makes it potentially useful in dynamic monitoring for industrial applications.

© 2019 Optical Society of America under the terms of the OSA Open Access Publishing Agreement

1. Introduction

Accelerometers (vibration sensors) have been widely incorporated in numerous applications such as in seismic exploration [1], navigation systems [2] and in industrial and health monitoring applications [3]. A variety of them exist and are specialized on specific applications. For example, accelerometers used in the detection of seismic waves are required to be sensitive to low frequencies (<100 Hz) [4] and in mechanical equipment such as rotating machinery and aero-engines, sensitive to high frequencies is required [5]. Besides the frequency factor, information on the orientation is another critical detail in vibration systems, such as cantilevered microwire [6]. Various approaches have been reported to achieve a high sensitivity and a dynamic range of frequency response. However, mechanical measurements in an acceleration system capable of distinguishing vector orientations remain challenging [7]. Generally, multiple single-axis accelerometers have been used to map the vibration directions, thereby, increasing the system complexity.

During the past two decades, fiber-optic accelerometers have attracted widespread interests due to their distinct advantages [8–10], e.g. capability of multiplexing and conducting distant measurements and immunity to electromagnetic interference. Generally, acceleration measurements can be carried out by detection of strain or displacement induced by the movement of the inertial mass attached to the sensor body. In the process of orientation determination, accelerometers vary according to their respective axes of vibration. The most fundamental accelerometers are single-axis, denoting their sensitivity to a single direction of vibration. For example, Cranch et al. has reported an accelerometer comprising a fiber coil embedded in an epoxy disk [11]. Using this design, the strain caused by acceleration has been measured by a Michelson interferometer. However, only the vibration which was vertical to

#365298 https://doi.org/10.1364/OE.27.020848
Journal © 2019 Received 17 Apr 2019; revised 22 May 2019; accepted 27 May 2019; published 11 Jul 2019

Optics EXPRESS

its plane caused the disk to flex. Villatoro et al. has introduced another interferometric sensor through splicing a segment of a strongly-coupled multi-core fiber (MCF) to a conventional single-mode fiber (SMF) [12]. The vibration waves have induced local pressure in the MCF, leading to a periodic shift of the interference pattern. Moreover, Rong et al. has demonstrated a fiber Bragg grating (FBG) based accelerometer in a depressed-cladding fiber [13] where acceleration measurements have been achieved from power detection of the fundamental core mode resonance.

In addition, there are several sensors designed as two-axis optical accelerometers, based on deflection of the sensing element, with its axis perpendicular to the applied acceleration. Fender et al. has proposed an accelerometer using FBGs inscribed in a four-core MCF to sense the strain difference between two cores [14]. When the vibration was normal to the plane formed by the two cores, FBGs in these two cores can only detect acceleration in a certain direction while the other two FBGs remained insensitive, and vice versa. Thus, such a sensor requires two pairs of FBGs to detect accelerations in two orthogonal directions. However, the actual vibration angle during random accelerations remains unexplored. Li et al. has combined two vibration sensors for detection of acceleration sensitivity in two dimensions [15], where a cantilever has been directly fabricated on the SMF itself to measure the deflection caused by vibration. Besides, Linessio et al. has implemented a biaxial optical accelerometer based on four FBGs placed in opposite positions [16], capable of detecting acceleration in two orthogonal directions, simultaneously. However, these structures are sophisticated to fabricate and control, and are sensitive only in two directions.

Recently, the fiber-optic two-dimensional vector accelerometer has greatly raised the research interests. The accelerometer can discriminate orientation in 360°, providing more directional information during vibration, especially when the vibration source is unknown [17]. In order to distinguish the vibration direction, Rong et al. has introduced an orientation-sensitive fiber-optic accelerometer based on tilted FBGs (TFBGs) inscribed in the cladding of a thin-core fiber [17]. Strong orientation dependent vibration measurements have been achieved by power detection of the cladding resonance. Moreover, Bao et al. has demonstrated another vector accelerometer based on output power detection of orthogonal FBGs in a multi-clad fiber [7]. However, both of these accelerometers indicate only an orientation dependent acceleration response over a range of 0-360° with the absence of actual vibration orientation at random accelerations. As a result, distinguishing both the orientation as well as the acceleration simultaneously, using a two-dimensional vector accelerometer remains challenging. In other words, information on both parameters should be obtained with the use of a two-dimensional accelerometer under random circumstances.

In this paper, we propose and demonstrate a two-dimensional vector accelerometer using FBGs inscribed in a seven-core MCF. The acceleration sensitivity is investigated by varying the vibration orientation from 0 to 180° in steps of 10°. The sensor shows a strong orientation dependence, making it suitable for distinction of the vibration direction. In particular, with the use of only two outer cores, orientation, acceleration as well as the frequency of the vibration can be measured simultaneously by monitoring the Bragg wavelength shifts of the FBGs. The measurement accuracy of distinguishing the vibration orientation varies from 0.127 to 2.888°, depending on the acceleration value. Additionally, the FBG inscribed in the central core can be used for temperature compensation. Moreover, the sensing performance in terms of the acceleration sensitivity and dynamic frequency range can be optimized through adjusting the structure of the accelerometer. Experimental results demonstrate that the proposed two-dimensional vector accelerometer is able to obtain acceleration and orientation concurrently, with the use of a single fiber.

2. Principle of acceleration and orientation measurement

Figure 1(a) shows the scanning electron microscopic (SEM) image of the seven-core MCF used for the accelerometer, including its central core and six outer cores. The diameters of the

Optics EXPRESS

cores and cladding are ~8 and ~150 μm, respectively. The fiber is bend insensitive owing to the low-index trench surrounding each core. The pitch *d* between two adjacent cores is ~42 μm, as shown in Fig. 1(b). Prior to FBG inscription, the seven-core MCF was loaded in a chamber with hydrogen under a pressure of 100 bar at a temperature of ~80 °C for 3 days to enhance its photosensitivity. The FBGs were inscribed in all seven cores simultaneously through laser beam scanning method, using a 213 nm solid-state laser (Xiton Photonics, Impress 213) together with the phase mask (Ibsen Photonics) technique. The scanning speed was 0.01 mm/s and the grating length was 10 mm. Schematic illustration of the FBGs inscribed in the seven core MCF is shown in Fig. 3(b).

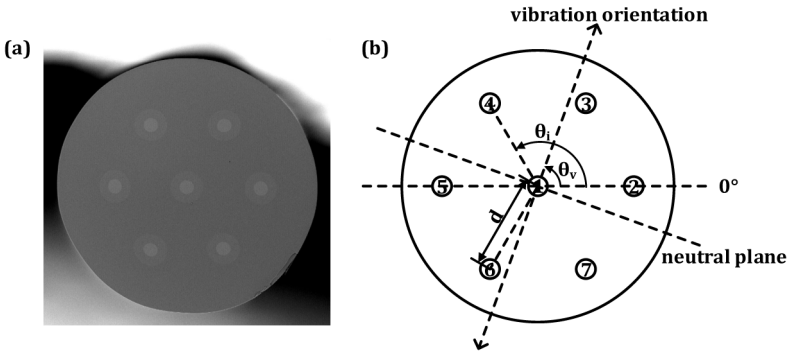

Fig. 1. (a) SEM image of the homogeneous seven-core MCF and (b) cross-section of the fiber cores with the defined geometrical parameters.

After FBG inscription, the seven-core MCF was spliced with a 7-to-1 fan-out using a fusion splicer (Fujikura, LZM-100). An interrogator (Micron Optics, sm130) with a wavelength resolution of 1 pm, was used to analyze the reflection spectra. Due to the symmetrical geometry of the cores, FBGs in three cores including the central core, together with two outer cores, which are not aligned in a straight line are sufficient to develop the accelerometer. The reason behind choosing the seven-core MCF together with the 7-to-1 fan-in/out device is due to their easy accessibility in the MCF range. Figure 2 shows the individual reflection spectra of the FBGs in the cores 1, 2, and 4.

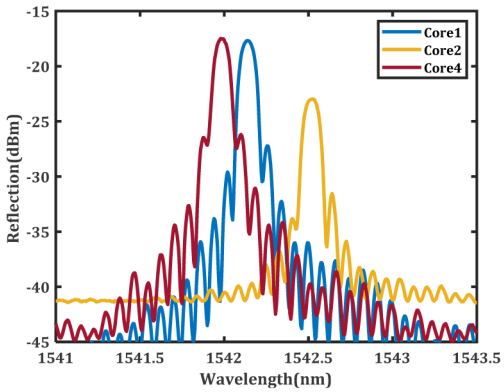

Fig. 2. Reflection spectra of the FBGs written in core 1, 2 and 4.

The basic principle of the FBG based accelerometer is to monitor the Bragg wavelength shifts of the gratings inscribed in different cores when vibration occurs. As shown in Fig. 2, it is evident that there is a slight difference in the central wavelengths of these cores, where λ_i (i = 1, 2, 4) for each core is 1542.14, 1542.52 and 1541.98 nm, respectively. This may result from the non-uniform UV exposure caused by the different spatial distribution of the cores

Optics EXPRESS

[18,19]. During the vibration process, the outer cores of the MCF, indicate a red shift in the Bragg wavelength when the fiber is stretched. On the contrary, a blue shift occurs when the core is compressed. However, the central core (i.e. core 1) is insensitive to vibration since its transversal position is located on the strain neutral plane at all times. Thus, the FBG in core 1 can be used for temperature compensation. As a result, the Bragg wavelength shift ($\Delta\lambda$) can be expressed by [20]

$$\Delta\lambda_i = (1 - p_e)\lambda_i \cdot \varepsilon_i, \tag{1}$$

where p_e is the effective photoelastic coefficient, relative to the effective index of the core and the Poisson's ratio of the fiber, and ε_i is the strain induced by the vibration on the i^{th} FBG, which can be described as [21]

$$\varepsilon_i = \frac{d_i}{R}\sin(\theta_v + \theta_i), \tag{2}$$

where d_i is the pitch between the outer core i (i.e. core 2-7) and core 1, as illustrated in Fig. 1(b). θ_v and θ_i indicate the orientation of vibration and angular position of each outer core i, respectively. R is the vibration-induced bending radius.

In order to obtain the vibration orientation and acceleration simultaneously in a single measurement, three FBGs in three individual cores, i.e. core 1, 2 and 4, were used to record the periodic change in strain during vibration. For vibrations that occur in random directions, the wavelength shifts of core 2 and 4 appear to have an opposite trend, if they are arranged at opposite sides of the neutral plane, which means one of them experiences a blue shift whereas the other experiences a red shift and vice versa. The wavelength shifts can be formulated as follows.

$$\frac{\Delta\lambda_2}{\lambda_2} = (1 - p_e)\frac{d_2}{R}\sin(\theta_v + \theta_2), \tag{3}$$

$$\frac{\Delta\lambda_4}{\lambda_4} = (1 - p_e)\frac{d_4}{R}\sin(\theta_v + \theta_4), \tag{4}$$

In these equations, θ_2 and θ_4 are obtained from Fig. 1(b) as 0 and $2\pi/3$, respectively. Pitch d remains the same for both cores, while R is much larger than d. Thereby, taking into account the values of maximum wavelength shifts of these FBGs at a certain acceleration, vibration orientation can be calculated from the following equation.

$$\theta_v = \arctan\left(\frac{\frac{\Delta\lambda_2}{\lambda_2}\sin\theta_4 - \frac{\Delta\lambda_4}{\lambda_4}\sin\theta_2}{\frac{\Delta\lambda_4}{\lambda_4}\cos\theta_2 - \frac{\Delta\lambda_2}{\lambda_2}\cos\theta_4}\right) \tag{5}$$

Once the orientation of vibration is determined, using the measured sensitivities under varying orientations, together with the wavelength shifts of the corresponding fiber cores, the acceleration value is identified. As a result, orientation and acceleration can be obtained simultaneously in a two-dimensional range.

3. Experimental setup and results

The experimental setup of the two-dimensional accelerometer is depicted in Fig. 3(c). The seven-core MCF with the inscribed FBGs is used as the sensing probe, which is fixed on a fiber rotator (Thorlabs, HFR007) to tune the vibration orientation from 0 to 180° in steps of 10°. A detailed illustration of the free-fiber is shown in Fig. 3(b), where the grating end is

Optics EXPRESS

placed 2 mm away from the fixed point of the rotator. Here, we define the orientation of 0° when core 2, 1 and 5 are maintained horizontal as shown in Fig. 1(b). According to the structure, length of the suspended fiber is vital, since it behaves as an inertial mass, which determines the resonance frequency. Afterwards, the accelerometer was mounted on the top of a shaker (Bruel & Kjaer, Type 4808) to characterize its performance. During the experiment, the shaker was excited by a sinusoidal-signal generator. The acceleration was increased up to 10 g (g = 9.8 m/s^2) with vibration frequencies ranging from 5 to 160 Hz. A high-resolution interrogator with a data acquisition rate of 2000 Hz was used to record the wavelength shifts of the three FBGs. Consequently, the vibration measurements were carried out under the conditions with various orientations, frequencies and acceleration values.

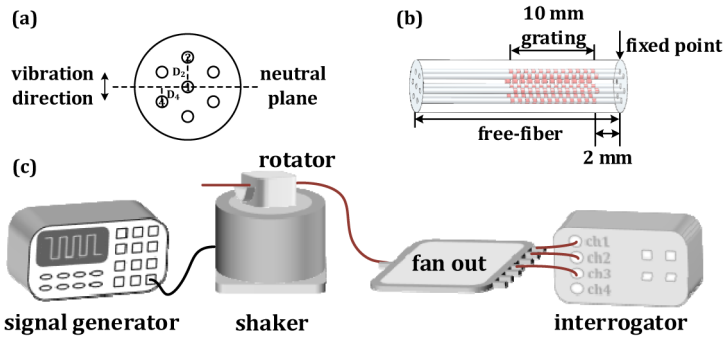

Fig. 3. (a) Definition of distance D from the core of interest to the neutral plane and (b) detailed illustration of the free-fiber with length L; (c) schematic setup for the vibration test of the two-dimensional accelerometer.

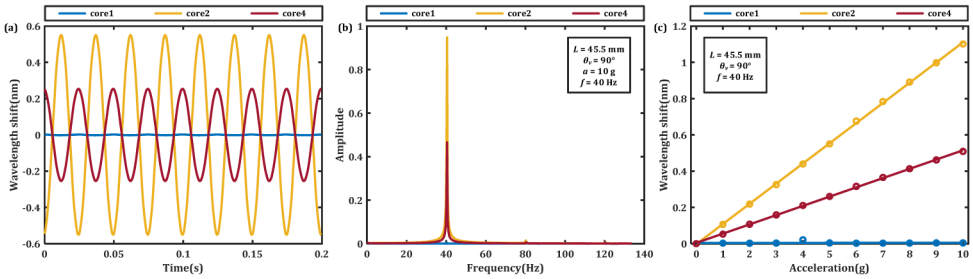

Fig. 4. (a) Real-time wavelength shifts of FBGs in core 1, 2 and 4 with the following values: L = 45.5 mm, f = 40 Hz, θ_v = 90° and a = 10 g. The corresponding (b) FFT spectrum with a = 10 g, and (c) wavelength shift versus applied acceleration at values from 0 g to 10 g.

In the experiment, a series of sine vibration waves with vibration frequencies ranging from 8 to 60 Hz was applied to the accelerometer with a free-fiber length L of 45.5 mm. During the test, the acceleration was increased from 0.2 g to 10 g for each frequency. Curves in Fig. 4(a) present the wavelength shifts of the FBGs in core 1, 2 and 4 in time domain, at vibration frequency f = 40 Hz, vibration orientation θ_v = 90° and acceleration value a = 10 g. From the results, it can be observed that the FBGs in core 2 and 4 experience an opposite wavelength shift since the neutral plane is located in between them. In addition, amplitude of the wavelength shift is dependent on the strain ε_i applied to each FBG during vibration, which is proportional to the distance D_i (i.e. i = 2 and 4) from the core of interest to the neutral plane, as shown in Fig. 3(a). In contrast to the vibration responses of the outer cores, FBG inscribed in the central core shows insensitivity to vibration because it lies on the neutral plane. Figure 4(b) demonstrates the fast Fourier transfer (FFT) spectra of the time-domain results shown in Fig. 4(a). The measured frequency matches well with the excited frequency from the signal generator. Furthermore, the maximum wavelength shifts as a function of the

Optics EXPRESS

applied accelerations are plotted for the scenario where, L = 45.5 mm, f = 40 Hz and θ_v = 90°, and the results are shown in Fig. 4(c). Slopes of the linear responses represent the measurement sensitivities under this condition for the three cores, which are 0.17 pm/g, 111.51 pm/g and 50.78 pm/g for core 1, 2 and 4, respectively.

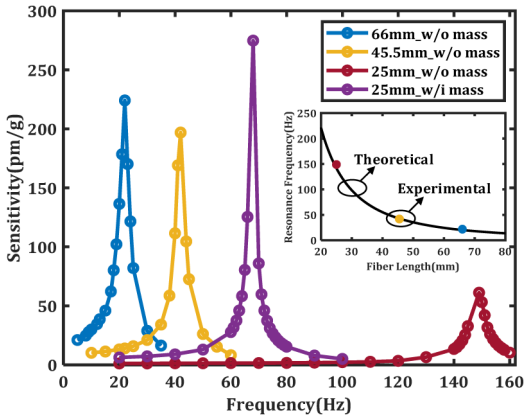

Fig. 5. Sensitivity-frequency responses of the FBG in core 2 when θ_v = 90°, L = 66, 45.5 and 25 mm with or without a glue mass. Inset shows the theoretical resonance frequencies under different fiber lengths.

In order to further investigate the performance of the accelerometer, the sensitivity-frequency response was considered, which can reflect the resonance frequency and the flat response range. Basically, the free-fiber length L can influence the resonance frequency significantly as the additional weight of the fiber functions as the inertial mass. The responses for three different L, i.e. 66, 45.5 and 25 mm, were characterized accordingly. The length between the grating end and the fixed point was kept at 2 mm for consistency during all the tests, as shown in Fig. 3(b), and L was shortened by cutting the free-fiber end. Figure 5 displays the vibration sensitivity versus the exciting frequency for the FBG in core 2 when θ_v is 90° under different L. When L is 66 mm as shown in the blue curve, a resonance frequency of 22 Hz appears in the range from 5 to 35 Hz, with a peak sensitivity of 224.1 pm/g. To increase the resonance frequency, L was shortened to 45.5 and then 25 mm. As a result, the resonance frequency appears at 42 and 149 Hz, with the peak sensitivities reduced to 196.9 and 61.19 pm/g, respectively. Meanwhile, theoretical resonance frequencies under different fiber lengths are plotted as shown in the inset in Fig. 5, together with the experimental results represented in corresponding colors. It is clearly observed that the experimental results of the resonance frequency measurements match well with the theoretically obtained results. However, there is a tradeoff between the sensitivity and the resonance frequency, which can be tuned according to the requirement of the application. One approach to increase the sensitivity at a relatively high frequency is to attach additional mass on the end of the free-fiber. As a demonstration, a small amount of glue was attached to the end of the free-fiber to increase the weight of the inertial mass. The sensitivity curve under same conditions is plotted in Fig. 5, which has a resonance frequency of 68 Hz and a peak sensitivity of 274.8 pm/g.

4. Orientation discrimination

The capability of orientation discrimination for the proposed two-dimensional accelerometer is investigated by applying different accelerations with various orientations. Due to the fact that wavelength shift is caused by the vibration-induced strain to individual FBG, the maximum shift relies on the distance from fiber core to the neutral plane, as shown in Fig. 3(a). Typically, the distance for a particular core (i.e. D_2) changes with the vibration orientation, signifying that the sensitivity varies periodically with the change of orientation.

Optics EXPRESS

When the fiber is rotated in different orientations over a range of 0-180°, D_2 and D_4 are different. Thus, the strain applied in these FBGs would change accordingly with different orientations, which can be distinguished by monitoring the wavelength shifts in the outer cores. Figure 6 shows the dependence of vibration sensitivity on the orientation of core 2 and 4 over a range of 0-180° in steps of 10°. Owing to the feature of vibration in one direction, the orientations with π differences are identical within 360° (e.g. 30° and 210°). Therefore, the orientation within 180° covers the entire two-dimensional plane. Figure 6(a) demonstrates the measured sensitivities with respect to the various orientations under the condition of L = 66 mm and f = 20 Hz, whereas Fig. 6(b) shows the results for the case of L = 45.5 mm and f = 40 Hz. As expected, at a certain orientation, the sensitivity is different for core 2 and 4. There is a phase shift between the results of core 2 and 4, i.e. 60°, which is the same as the geometrical angle between these two cores and the central core.

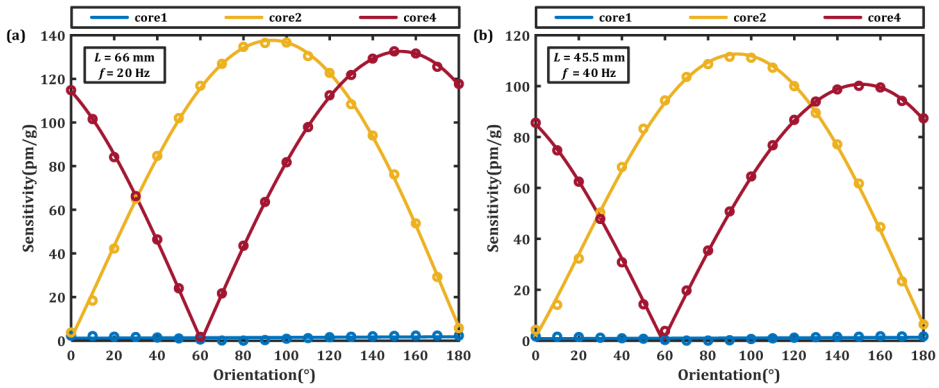

Fig. 6. Orientation dependence of the sensitivities of FBGs in core 1, 2 and 4 under different conditions. (a) L = 66 mm and f = 20 Hz; (b) L = 45.5 mm and f = 40 Hz.

It is possible that the same wavelength shift can be measured for the cases with different accelerations and orientations. As for an unknown vibration, information on its frequency, acceleration as well as the orientation should be extracted simultaneously from a single accelerometer by detecting the wavelength shifts of the FBGs. It is easy to obtain the frequency by conducting the FFT from the time-domain wavelength shifts. Then the acceleration can be obtained by referring to the calibrated sensitivities in Fig. 6 if the orientation is known in advance. According to Eq. (5), vibration orientation θ_v can be computed from the maximum wavelength shifts of two FBGs and their relative positions. Figure 7 shows the results of the orientation discrimination for the scenario of L = 45.5 mm and f = 30 Hz. The fitting line of the experimental results is plotted, together with the measured values under different vibration orientations. It can be seen that the measured orientation values stay consistent with the set values. Different accelerations from 1 g to 10 g at certain orientations are characterized, with the result under 60° shown in the inset. The error bars represent the orientation accuracy, which is defined by the absolute difference between the set values and the reconstructed values. Results show that the vibration direction can be achieved regardless of the acceleration, with accuracy ranges from 0.127 to 2.888° in 0-180° range, depending on the accelerations. From the magnified figure, a relatively low accuracy is found at high accelerations, which may be attributed to the fact that the free-fiber is slightly away from the vibration plane. However, it is insignificant for small accelerations. For a certain orientation value, e.g. 60°, the measured one is supposed to be the same. However, it is noted that there is an offset between the ideal and the measured ones obtained from the fitting line, which is calculated to be 1.75°. The offset value is probably caused when mounting the accelerometer to a certain orientation (e.g. 0°), which can be avoided if the mounting process controlled precisely.

Optics EXPRESS

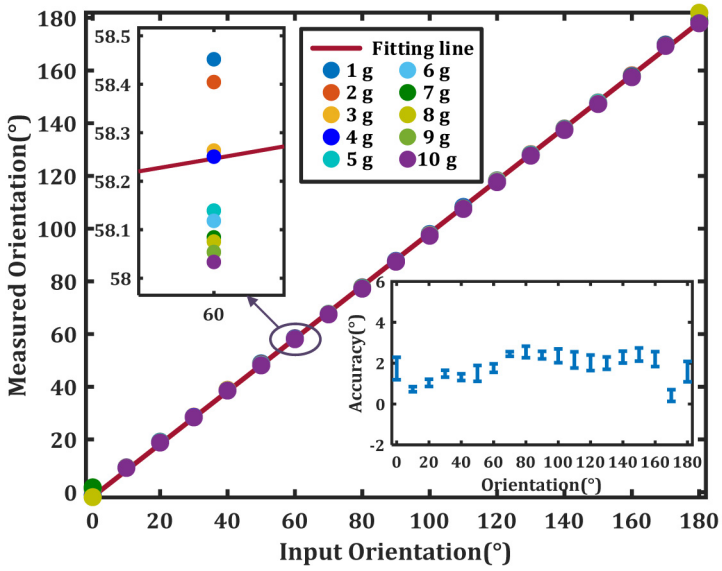

Fig. 7. Input and measured orientation values under specific orientations from 0 to 180° when L = 45.5 mm and f = 30 Hz. Inset shows the corresponding accuracy ranges.

5. Conclusion

In summary, we have proposed and demonstrated a novel two-dimensional accelerometer which has the ability to distinguish the value of orientation and acceleration simultaneously. A seven-core MCF with 10-mm long FBGs inscribed in the cores was used as an inertial mass to be the accelerometer probe, which is immune to temperature fluctuations since the central core stays on the neutral plane at all times during vibration. The maximum resonance frequency was measured at 149 Hz, which can be optimized by adjusting the free-fiber length and weight. Through monitoring the wavelength shifts of only three cores, including the central and two outer cores which are not aligned in a straight line, vibration orientation can be obtained with an accuracy range of 0.127 to 2.888°, which can be improved when orientation-sensitive factors are considered. With the use of this structure, orientation information as well as the acceleration can be obtained in a single fiber concurrently. Furthermore, the compact size of the sensor is beneficial for orientation-sensitive acceleration measurement applications.

Funding

The Hong Kong Polytechnic University (1-ZVGB, 1-BBYE, and 1-BBYS); National Natural Science Foundation of China (NSFC) 61827820).

References

1. A. Bertolini, R. DeSalvo, F. Fidecaro, M. Francesconi, S. Marka, V. Sannibale, D. Simonetti, A. Takamori, and H. Tariq, "Mechanical design of a single-axis monolithic accelerometer for advanced seismic attenuation systems," Nucl. Instrum. Methods Phys. Res. Sect. A-Accel. Spectrom. Dect. Assoc. Equip. **556**(2), 616–623 (2006).
2. C. W. Tan and S. Park, "Design of accelerometer-based inertial navigation systems," IEEE Trans. Instrum. Meas. **54**(6), 2520–2530 (2005).
3. J. W. Borinski, C. D. Boyd, and J. A. Dietz, "Fiber optic sensors for predictive health monitoring," in Proc. IEEE Autotestcon 250–**262** (2001).
4. Y. Weng, X. Qiao, T. Guo, M. Hu, Z. Feng, R. Wang, and J. Zhang, "A robust and compact fiber Bragg grating vibration sensor for seismic measurement," IEEE Sens. J. **12**(4), 800–804 (2012).
5. X. Wang, Y. Guo, L. Xiong, and H. Wu, "High-frequency optical fiber Bragg grating accelerometer," IEEE Sens. J. **18**(12), 4954–4960 (2018).

Optics EXPRESS

6. C. Fu, W. Zhu, W. Deng, F. Xu, N. Wang, L. Zou, and F. Xue, "Measuring the orientation of the flexural vibrations of a cantilevered microwire with a micro-lens fiber-optic interferometer," Appl. Phys. Lett. **113**(24), 243101 (2018).
7. W. Bao, X. Qiao, and Q. Rong, "Fiber-optic vector accelerometer using orthogonal Bragg grating inscription over innermost cladding of a multi-clad fiber," J. Lightwave Technol. **37**(11) 2706–2712 (2018).
8. Y. R. García, J. M. Corres, and J. Goicoechea, "Vibration detection using optical fiber sensors," J. Sens. **2010**, 1 (2010).
9. T. K. Gangopadhyay, "Prospects for fiber Bragg gratings and Fabry-Perot interferometers in fiber-optic vibration sensing," Sensor Actuat. A-Phys. **113**(1), 20–38 (2004).
10. M. D. Todd, G. A. Johnson, B. A. Althouse, and S. T. Vohra, "Flexural beam-based fiber Bragg grating accelerometers," IEEE Photonics Technol. Lett. **10**(11), 1605–1607 (1998).
11. G. A. Cranch and P. J. Nash, "High-responsivity fiber-optic flexural disk accelerometers," J. Lightwave Technol. **18**(9), 1233–1243 (2000).
12. J. Villatoro, E. Antonio-Lopez, J. Zubia, A. Schülzgen, and R. Amezcua-Correa, "Interferometer based on strongly coupled multi-core optical fiber for accurate vibration sensing," Opt. Express **25**(21), 25734–25740 (2017).
13. Q. Rong, T. Guo, W. Bao, Z. Shao, G. D. Peng, and X. Qiao, "Highly sensitive fiber-optic accelerometer by grating inscription in specific core dip fiber," Sci. Rep. **7**(1), 11856 (2017).
14. A. Fender, W. N. MacPherson, R. R. J. Maier, J. S. Barton, D. S. George, R. I. Howden, G. W. Smith, B. J. S. Jones, S. McCulloch, X. F. Chen, R. Suo, L. Zhang, and I. Bennion, "Two-axis temperature-insensitive accelerometer based on multicore fiber Bragg gratings," IEEE Sens. J. **8**(7), 1292–1298 (2008).
15. J. Li, G. Y. Wang, J. N. Sun, R. R. J. Maier, W. N. Macpherson, D. P. Hand, and F. Z. Dong, "Micro-machined optical fiber side-cantilevers for acceleration measurement," IEEE Photonics Technol. Lett. **29**(21), 1836–1839 (2017).
16. R. P. Linessio, K. D. M. Sousa, T. D. Silva, C. A. Bavastri, P. F. D. C. Antunes, and J. C. C. D. Silva, "Induction motors vibration monitoring using a biaxial optical fiber accelerometer," IEEE Sens. J. **16**(22), 8075–8082 (2016).
17. Q. Rong, X. Qiao, T. Guo, W. Bao, D. Su, and H. Yang, "Orientation-dependent fiber-optic accelerometer based on grating inscription over fiber cladding," Opt. Lett. **39**(23), 6616–6619 (2014).
18. M. Hou, K. Yang, J. He, X. Xu, S. Ju, K. Guo, and Y. Wang, "Two-dimensional vector bending sensor based on seven-core fiber Bragg gratings," Opt. Express **26**(18), 23770–23781 (2018).
19. E. Lindley, S. S. Min, S. Leon-Saval, N. Cvetojevic, J. Lawrence, S. Ellis, and J. Bland-Hawthorn, "Demonstration of uniform multicore fiber Bragg gratings," Opt. Express **22**(25), 31575–31581 (2014).
20. A. D. Kersey, M. A. Davis, H. J. Patrick, M. LeBlanc, K. P. Koo, C. G. Askins, M. A. Putnam, and E. J. Friebele, "Fiber grating sensors," J. Lightwave Technol. **15**(8), 1442–1463 (1997).
21. R. S. Chang and P. E. Dupont, "FBG-based shape sensing tubes for continuum robots," in Proc. IEEE Int. Conf. Robot. Autom. 3531–3537 (2014).

138.132.161.52 {ts '2019-09-03 21:49:16'}